Int. J. Electrochem. Sci., 7 **(2012)** 10121 - 10131

International Journal of
ELECTROCHEMICAL
SCIENCE
www.electrochemsci.org

Experimental and Theoretical Study for Corrosion Inhibition of Mild Steel by L-Cysteine

Hui Cang[1,*], *Zhenghao Fei*[2], *Wenyan Shi*[1,3], *Qi Xu*[1]

[1] College of chemical engineering and biological, Yancheng institute of technology, Yancheng 224051, China
[2] Jiangsu Provincial Key Laboratory of Coastal Wetland Bioresources and Environmental Protection, Yancheng Teachers University, Yancheng 224002, China
[3] The Institute of Chemistry &Technology, Nanjing University of Science & Technology, Nanjing 210094, China
[*]E-mail: Canghui_ycit@126.com; Canghui@ycit.edu.cn

Received: 23 August 2012 / *Accepted:* 12 September 2012 / *Published:* 1 October 2012

The corrosion inhibition of mild steel in 1M HCl and 0.5M H_2SO_4 by L-Cysteine (Cys) has been studied using electrochemical impedance spectroscopy (EIS) measurements and molecular dynamics (MD) simulation. The results show that the inhibition efficiency increase with the increase of Cys concentration in both acids, and the higher inhibition efficiency is obtained in 1 M HCl. The adsorption of Cys molecules on the mild steel surface obeys Langmuir adsorption isotherm in both acids, and occurs spontaneously. The MD simulation results show that with the adsorption of chloride ions has the higher negative interaction energy comparing to the case of the adsorption of sulfate ions in the Fe + anion + Cys simulated system.

Keywords: L-Cysteine, Mild steel, EIS, Interface, Modelling studies

1. INTRODUCTION

It is well known that acid solutions are generally used for the removal of undesirable scale and rust in several industrial processes. Acid solutions are extensively used, the most important of which are acid picking, industrial acid cleaning, acid-descaling and oil well acidizing. The commonly used acids are hydrochloric acid and sulphuric acid. Since acids are aggressive, inhibitors are usually used to minimize the corrosive attack on metallic materials. Use of inhibitors is one of the most practical methods for protection against corrosion especially in acid solutions to prevent metal dissolution and acid consumption [1].

Large mumber of organic compounds were studied to investigate their corrosion inhibition potential. For example, the effect of organic nitrogen compounds on the corrosion behavior of iron and steel in acidic solutions are usually employed for their rapid action [2-5]. However, unfortunately, most of these compounds are not only expensive but also toxic to both human being and environment. The toxic effects of these inhibitors have led to the use of naturally occurring products as corrosion inhibitors. The plant extracts thus emerge out as are viewed as an incredibly rich source of naturally synthesized chemical compounds that can be extracted by simple procedures with low cost and are biodegradable in the environment. The extract of *Zenthoxylum alatum* [6], *Damsissa* [7], *Phyllanthus amarus* [8], *Murraya koenigii* [9], *Oxandra asbeckii* [10], *Asteriscus Graveolens* [11] and *Stevia rebaudiana* [12] etc., were found to display strong inhibition for steel corrosion in acid solutions.

As is well known, the plant extract is a complex mixture of various phytochemical components. Amino acids is one of the important constituent in this family which act as the role of the inhibitor for the metal corrosion [13]. In recent years many amino acids were reported as good safe corrosion inhibitors for metals in various aggressive media [14-17]. The existing results show that most of amino acids act by adsorption on the metal surface. The adsorption of inhibitors takes place through nitrogen, oxygen and sulphur heteroatoms.

In this respect, and in a continuation of our program, the present work devotes to investigate the adsorption and corrosion inhibition of L-Cysteine (Cys) on mild steel in 0.5 M H_2SO_4 and 1.0 M HCl by electrochemical impedance spectroscopy (EIS). It was also the purpose of this work to employ molecular dynamics (MD) to discuss the adsorption mode of Cys molecule and electrolyte anions on the Fe (001) surface, and to explain or rationalize experimental studies.

2. EXPERIMENTAL

2.1 Electrochemical measurements

The electrolyte was 0.5M H_2SO_4 and 1M HCl with vatious concentrations of Cys. Reagent-grade H_2SO_4 and HCl were used, and the aggressive solution were made up with double-distilled water. The working electrode is A_3 mild steel rod (C, 0.17%; Si, 0.20%; Mn, 0.37%; S, 0.03%; P, 0.01% and reminder iron). The rod specimen was embedded in Teflon holder using epoxy resin with an exposed area of 0.785 cm^2.

A traditional three-electrode cell was used for electrochemical measurements. A platium sheet (1.0 cm^2) electrode was used for the auxiliary electrode, and the reference electrode was a saturated calomel electrode (SCE) with a Luggin capillary. All potentials were measured with respect to the SCE. The experiments were conducted at 25 ± 2 ℃ using a water bath temperature-controlled. Volumes of the acid solution were 150 cm^3 in all experiments. Before each experiment, the electrode was first mechanically polished with various grades of sandpaper (up to 1200 grit) and then ultrasonically cleaned in acetone for 2 min, followed by a rinse in double-distilled water.

Electrochemical experiments were carried out using a CHI660B electrochemical workstation. Electrochemical impedance spectroscopy (EIS) measurements were carried out at open-circuit

potential over a frequency range of 0.1 Hz - 100 kHz. The sinusoidal potential perturbation was 5 mV in amplitude. Electrochemical data were obtained after 1 h of immersion with the working electrode at the rest potential, and all tests have been performed in non-de-aerated solutions under unstirred conditions. Electrochemical data were analyzed by a Zsimpwin 3.30 Demo Version software.

2.2 Molecular dynamics simulations

The molecular dynamics (MD) simulations were performed using the Materials Studio software. Fe (110) surface was chosen for the simulation study. The MD simulation of the interaction between molecular Cys and Fe (110) surface was carried out in a simulation box (14.33 Å × 14.33 Å × 28.66 Å) with periodic boundary conditions to model a representative part of the interface devoid of any arbitrary boundary effects. The iron substrate with (110) plane was first optimized to minimum energy, then the addition of the Cys molecule near to the surface was carried out and the behavior of the Cys molecule on the Fe (110) surface was simulated using the compass force field. The MD simulation was performed under 298 K, NVT ensemble, with a time step of 0.1 fs and simulation time of 50 ps. The interaction energy $E_{\text{interaction}}$ between the iron surface and the Cys molecule was calculated as follows:

$$E_{\text{interaction}} = E_{\text{total}} - (E_{\text{surface}} + E_{\text{Cys}}) \quad (1)$$

where E_{total} is the total energy of iron crystal together with the adsorbed Cys molecule, E_{surface} and E_{Cys} are the energy of the iron crystal and free Cys molecule, respectively. Considering that the anions (i.e., chloride or sulfate ions) in the solutions could adsorb on the iron surface, the MD simulation was also performed in the box containing the adsorption of the anions. Here, the interaction energy $E_{\text{interaction}}$ was calculated according to the following equation:

$$E_{\text{interaction}} = E_{\text{total}} - (E_{\text{surface}} + E_{\text{ion}} + E_{\text{Cys}}) \quad (2)$$

where E_{ion} is the energy of chloride or sulfate ions. Semi-empirical PM3 method from the program package MOPAC2007 was also used to optimize the geometry structure of Cys molecule, and the charges of all N and S atoms of the molecule were calculated. The binding energy of the inhibitor molecule is the negative value of the interaction energy, namely:

$$E_{\text{binging}} = - E_{\text{interaction}}$$

3. RESULTS AND DISCUSSION

3.1 Electrochemical impedance spectroscope (EIS)

Figs. 1 and 2 illustrate the Nyquist diagrams for Cys in 1.0 M HCl and 0.5M H_2SO_4 at 25 ± 2 ℃, respectively. These diagrams show single capacitive loop in both acids, which is attributed to

charge transfer of the corrosion process [18], and the diameters of the loops increase with the increase of Cys concentration. The capacitive loops in both acids are not exact semicircles but depressed to some extent which can be attributed to the frequency dispersion effect as a result of the roughness and inhomogeneous of electrode surface [19]. Furthermore, the diameter of the capacitive loop in the presence of inhibitor is larger than that in the absence of inhibitor (blank solution), and increases with the inhibitor concentration. This indicates that the impedance of inhibited substrate increase with the inhibitor concentration.

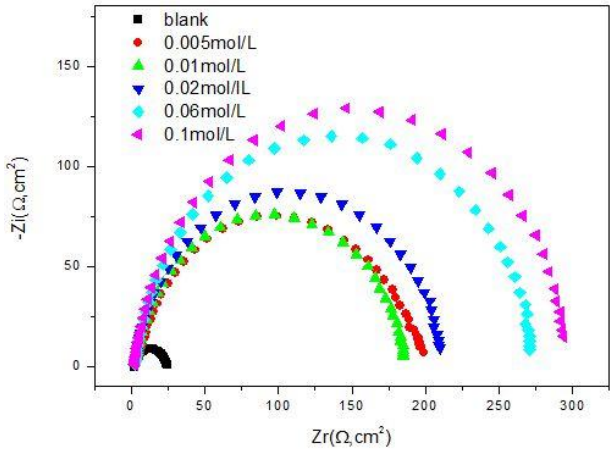

Figure 1. Nyquist plots of the corrosion of Cys in 1.0 M HCl without and with different concentrations of Cys at 25 ± 2 ℃ (immersion time is 1 h).

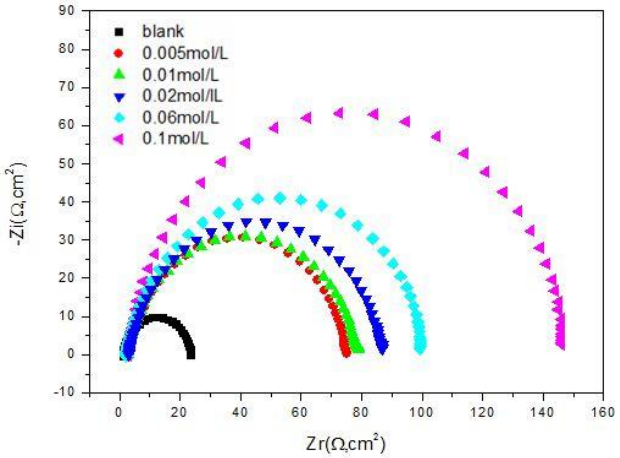

Figure 2. Nyquist plots of the corrosion of Cys in 0.5M H_2SO_4 without and with different concentrations of Cys at 25 ± 2 ℃ (immersion time is 1 h).

In the evaluation of Nyquist plots, the difference in real impedance at lower and higher frequencies is generally considered as charge-transfer resistance. The resistance between the metal and outer Helmholtz plane (OHP) must be equal to the R_{ct}. The impedance data are analyzed using the circuit in Fig. 3, in which R_s represents the electrolyte resistance, R_{ct} the charge-transfer resistance. According to Fig.3, the charge-transfer resistance, which corresponds to the diameter of Nyquist plot,

used to determines the corrosion inhibition and represents the resistance between the metal/OHP (outer Helmholtz plane). Fig. 3 describes the potential distributions on the metal/solution interface and proposed electrical equivalent circuit diagram for the corrosion system blank solution. It is worth mentioning that the double layer capacitance (C_{dl}) value is affected by imperfections of the surface, and that this effect is simulated via a constant phase element (CPE) [20]. From Fig. 1 and 2, the impedance loops measured are depressed semi-circles with their centers below the real axis, where the kind of phenomenon is known as the "dispersing effect" as a result of the roughness and other inhomogeneities of the electrode surface, thus one constant phase element (CPE) is substituted for the capacitive element to give a more accurate fit.

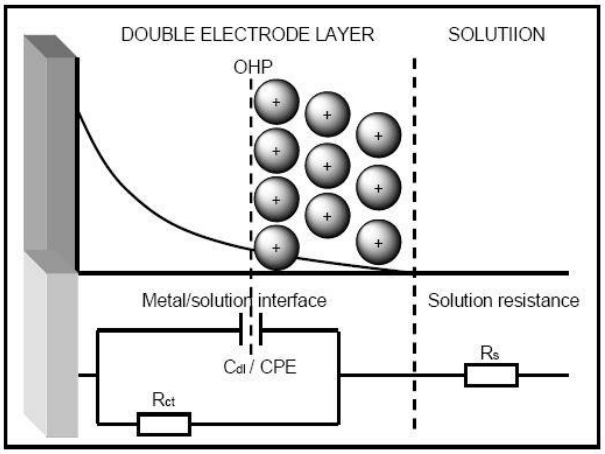

Figure 3. Equivalent circuit used to model impedance data in the acid solutions. OHP, outer Helmholtz plane; R_s, solution resistance; R_{ct}, charge-transfer resistance; C_{dl}, double layer capacitance.

The impedance of a constant phase element is described by the expression:

$$Z_{CPE} = Y_0^{-1}(j\omega)^{-n}$$

where Y_0 is a proportional factor, n has the meaning of a phase shift. For n=0, CPE represents a resistance, for n=1 a capacitance, for n=0.5 a Warburg element and for n=-1 an inductance. According to Hsu and Mansfeld [21], the value of the double-layer capacitance (C_{dl}) can be obtained from the equation:

$$C_{dl} = Y_0(\omega^{''})^{n-1}$$

where $\omega^{''}$ is the frequency at which the imaginary part of the impedance has a maximum.

The impedance parameters such as solution resistance (R_s), charge transfer resistance (R_{ct}), double-layer capacitance (C_{dl}) and inhibition efficiency (η, %) are listed in Table 1. The values of η are calculated by the charge transfer resistance as follows:

$$\eta(\%) = \frac{R_{ct} - R_{ct}^{0}}{R_{ct}} \times 100$$

where R_{ct} and R_{ct}^{0} are the charge transfer resistance in presence and absence of inhibitor, respectively.

Table 1. Fitting the EIS for mild steel in both acids containing different concentration of Cys.

Acids	C_{inh} /mol·L^{-1}	R_s / Ω cm^2	R_t / Ω cm^2	C_{dl} / μF cm^{-2}	η / %
1.0 M HCl	Blank	2.306	28.70	87.87	-
	0.005	2.222	194.1	80.28	84.49
	0.01	4.071	211.9	74.06	85.21
	0.02	2.141	274.3	70.93	86.46
	0.06	2.078	285.0	69.42	89.54
	0.1	2.193	298.9	69.25	90.40
0.5 M H_2SO_4	Blank	1.664	21.88	172.46	-
	0.005	3.401	72.38	119.91	69.77
	0.01	2.105	76.32	121.06	71.38
	0.02	3.309	84.54	135.24	74.12
	0.06	2.704	99.32	140.66	77.44
	0.1	2.573	146.0	155.83	85.01

It is clear from Table 1 that by increasing the inhibitor concentration, the C_{dl} values trend to decrease and the inhibition efficiency increases. According to the Helmholtz model [22]:

$$\delta_{org} = \frac{\varepsilon_0 \varepsilon_r}{C_{dl}}$$

where δ_{org} is the thickness of the protective layer, ε_0 is the dielectric constant and ε_r is the relative dielectric constant. Therefore, the decrease in the C_{dl}, which can result from a decrease in local dielectric constant and/or an increase in the thickness of the electrical double layer, suggests that the inhibitor molecules functions by adsorption at the metal/solution interface as a consequence of replacement of water molecules by the extract compounds [23]. η (%) increases with increases of the concentration of Cys, and follows the order: η (%) (HCl) > η (%) (H_2SO_4). The maximum η (%) values are 90.4% and 85.0% in 1.0 M HCl and 0.5 M H_2SO_4, respectively. These results confirm that Cys exhibits good inhibitive performance for mild steel in both acid solutions, and it is more efficient to inhibit the corrosion of steel in 1.0 M HCl than 0.5 M H_2SO_4.

3.2 Molecular dynamics sumulations

The MD simulations is first performed to study the adsorption behavior of Cys molecule on the Fe (110) surface without the adsorption of the solvent anions (Fe + Cys system). After the system reaches equilibrium, criterion of which is that both temperature and energy are carried out to obtain E_{total}, $E_{surface}$ and E_{Cys}, and then $E_{interaction}$ can be calculated from equation (1). The equilibrium geometry structure of Cys is similar to the planar structure obtained from the geometry optimization using PM3 method.

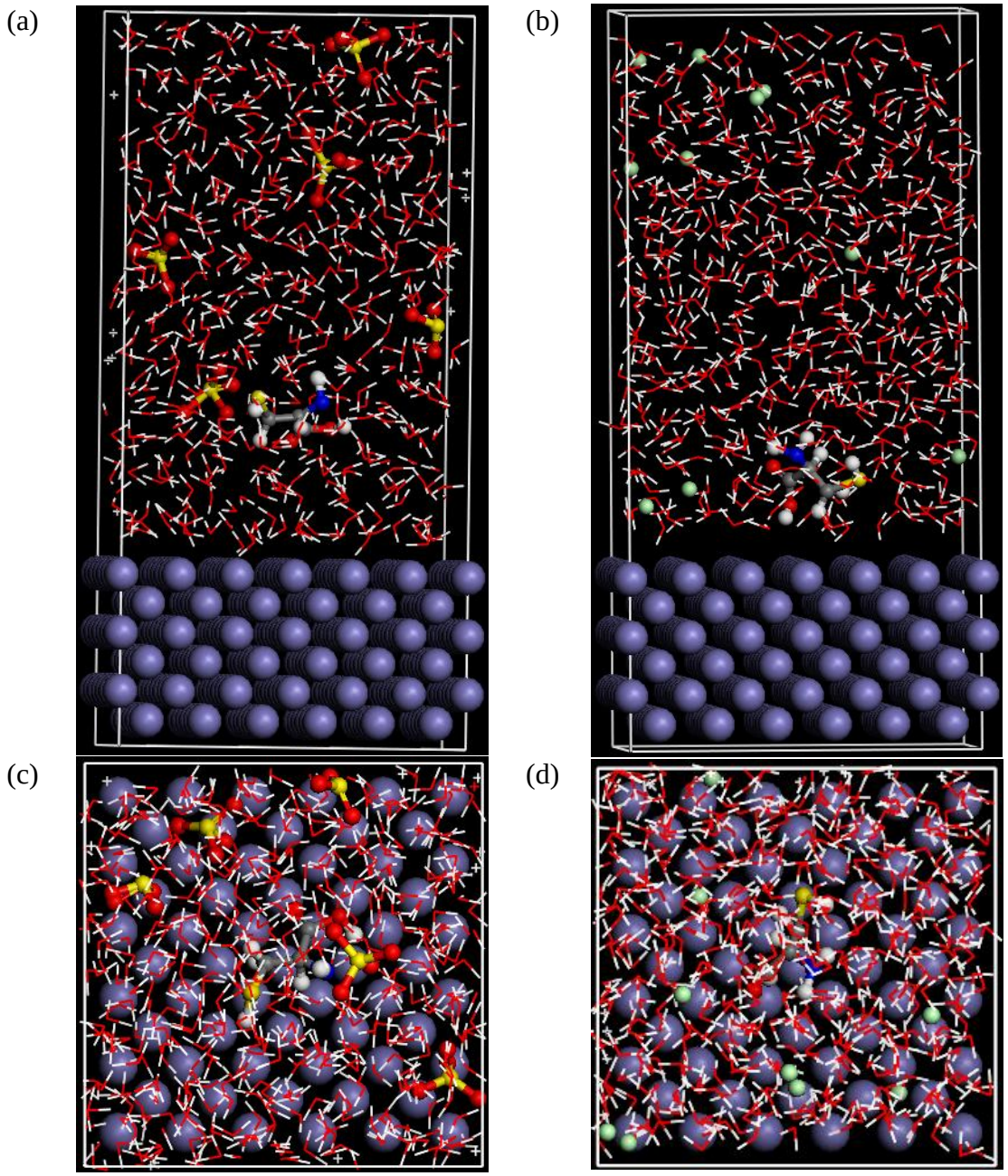

Figure 4. Results of the MD of (a) side view of Fe + SO_4^{2-} + Cys, (b) vertical view of Fe + SO_4^{2-} + Cys, (c) side view of Fe + Cl^- + Cys, (d) vertical view of Fe + Cl^- + Cys.

The planar molecule adsorbs on the Fe (110) surface in almost parallel manner, which is attributed to the interaction between Cys molecule and iron surface. However, in acidic solution containing some anions, such as chloride or sulfate ions, adsorption of organic molecules is not always a direct combination of the molecule with the metal surface [24]. The specific adsorption of anions having a smaller degree of hydration is expected to be more pronounced, namely, the anions will be first to get adsorbed on the metal surface [23]. In some cases, the adsorption of organic molecules can occur through the already adsorbed chloride or sulfate ions, which interfere with the adsorbed organic molecules [16]. In order to simulate the influence of the nature of anion on the adsorption of Cys molecule on both acids, chlorides or sulfates are first added near to the Fe (110) surface, and Cys molecule is added near to the anion layer (Fe +anion +Cys system), and then the MD simulation of the system is performed.

The close contacts between Cys, anions and iron surface as well as the best adsorption configuration for the compound are shown in Fig. 4. With the adsorption of sulfate ions the structure plane of Cys molecule is vertical to the iron surface, and in the case of chloride ions the plane is approximately vertical to the iron surface, too. Being specifically adsorbed, the anions create an excess negative charge towards the solution. Hence S atom of Cys, which carries positive charge, can easily adsorb on the surface created by the anions through the electrostatic interaction, while N atoms, which carry negative charges, will be repulsed away from the surface. The calculated $E_{interaction}$ of Fe + anion + Cys system are shown in Table 2. The higher the negative values of interaction energy, the easier inhibitor adsorbs on the surface, the higher the inhibition efficiency [25]. It can be seen from Table 2 that with the adsorption of chloride ions Cys gives the higher negative interaction energy comparing to that with the adsorption of sulfate ions. Therefore, in chloride acid solution, in which chloride ions adsorbed on the iron surface, Cys gives the higher inhibition efficiency. Obviously, the simulation result is consistent with the EIS experimental result. Because Cys is organic acid, Cys molecule may exist as protonated form through nitrogen atoms and/or acetate radical in acidic solution. Hence, the interaction between the metal surface and the protonated form of Cys will be further studied.

Table 2. Interaction energies from molecular dynamics simulations.

Systems	$E_{interaction}$ / kJ mol^{-1}	$E_{binding}$ / kJ mol^{-1}
Fe + Cys	-497.0	497.0
Fe + Cys + SO_4^{2-}	-539.9	539.9
Fe + Cys + Cl^-	-1437.3	1437.3

3.3 Adsorption isotherm

The type of the adsorption isotherm can provide additional information about the properties of the tested compounds. For this purpose, the values of surface coverage (θ) corresponding to different concentrations of Cys extract have been used to determine the adsorption isotherm. Calculation of the

coverage from the EIS experiment data C_{dl} is the method used widely according to the following equation:

$$\theta = \frac{C_{dl(\theta=0)} - C_{dl,\theta}}{C_{dl(\theta=0)} - C_{dl(\theta=1)}}$$

where $C_{dl(\theta=0)}$ and $C_{dl(\theta=1)}$ are the double layer capacitances of the inhibitor-free and entirely inhibitor-covered surfaces, respectively. $C_{dl,\theta}$ is the composite total double layer capacitance for any intermediate coverage θ. Several adsorption isotherms, such as Langmuir, Temkim and Frumkin isotherms, have been tested for the description of adsorption behavior of the inhibitor. The plots of C_{inh}/θ against C_{inh} give straight lines with the slope of 0.989 and 1.279 in 1 M HCl and 0.5 M H_2SO_4, and the value of correlation coefficient in 1 M HCl and 0.5 M H_2SO_4 are 0.992 and 0.999, respectively (Fig. 5).

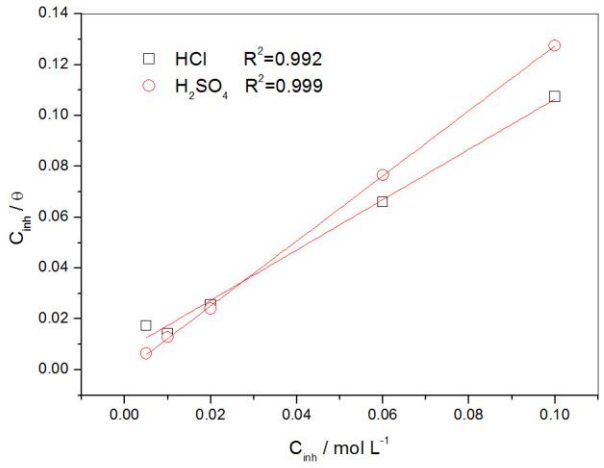

Figure 5. Langmuir adsorption isotherm plots for the adsorption of Cys in 1 M HCl and 0.5 M H_2SO_4 on the surface of mild steel.

The results indicate that obeys the Langmuir adsorption isotherm on the mild steel surface in both acids:

$$\theta = \frac{KC_{inh}}{1 + KC_{inh}}$$

where K is the equilibrium constant of the adsorption process. The free energy of adsorption processs ΔG^0_{ads} can be calculated from the equation [14]:

$$K = \frac{1}{55.5}\exp(\frac{-\Delta G^0_{ads}}{RT})$$

The value of ΔG^0_{ads} from the Langmuir adsorption isotherm in 1 M HCl and 0.5 M H_2SO_4 were calculated to be -29.5 kJ mol^{-1} and -22.7 kJ mol^{-1}, respectively . The large negative values of ΔG^0_{ads} indicate adsorption of Cys is spontaneous in both acids [19]. Generally, values of ΔG^0_{ads} around -20 kJ mol^{-1} or lower are consistent with the electrostatic interaction between the charged molecules and the charged metal (physisorption); those around -40 kJ mol^{-1} or higher involve charge sharing or charge transfer from organic molecules to the metal surface to form a coordinate type of bond (chemisorption) [22]. The calculated ΔG^0_{ads} value shows, therefore, that the adsorption mechanism of Cys on steel involves both two types of interaction. Indeed, due to the strong adsorption of water molecules on the surface of mild steel, one may assume that adsorption occurs first due to the physical force. The removal of water molecules from the surface is accompanied by chemical interaction between the metal surface and adsorbate, and that turns to chemisorptions [12]. In sum, the large negative values of ΔG^0_{ads} reveal that the adsorption process takes place spontaneously and the adsorbed layer on the surface of mild steel is highly stable [25]. This is in good agreement with the results obtained from molecular dynamics sumulations.

4. CONCLUSIONS

The L-Cysteine (Cys) inhibits the corrosion of mild steel in 1 M HCl and 0.5 M H_2SO_4 solutions, but the better performance has been found in the case of 1 M HCl. Inhibition efficiencies increases by increasing the inhibitor concentration in both acids with the EIS studies. Adsorption of Cys on the mild steel surface is spontaneous and obeys the Langmuir isotherm. The molecular dynamics simulation results reveal that Cys molecules adsorb on the iron surface in the vertical manner with the adsorption of the electrolyte anions, and the higher negative interaction energy is obtained in the case of adsorption of chloride ions.

ACKNOWLEDGEMENT
This work was funded by the Applied Basic Research Project of Yancheng Institute of Technology of Chian, Jiangsu (Grant no. XKR2011005) and Jiangsu Beach Biological Resources and Environmental Protection of key Construction Laboratory Funding (JLCBE11002). The authors acknowledge Dr. Jinling Shao, from School of Chemistry and Chemical Engineering, Nanjing University of Technology in computational calculations.

References

1. L.R. Chauhan, and G. Gunasekaran, *Corros. Sci.*, 49 (2007) 1143.
2. L. M. Vracar and D. M. Drazic, *Corros. Sci.*, 44 (2002) 1669.
3. M. Behpour, S. M. Ghoreishi, N. Soltani and M. Salavati-Niasari, *Corros. Sci.*, 51 (2009) 1073.
4. Y. M. Tang, X. Y. Yang, W. Z. Yang, R. Wan, Y. Z. Chen and X. S. Yin, *Corros. Sci.*, 52 (2010) 1801.
5. H. Cang, W. Y. Shi, J. L. Shao and Q. Xu, *Int. J. Electrochem. Sci.*, 7 (2012) 5626.
6. L.R. Chuanhan and G. Gunasekaran, *Corros. Sci.*, 49 (2007) 1143.

7. A. M. Abdel-Gaber, B. A. Abd-El Nabey, I. M. Sidahmed, A. M. El-Zayady and M. Saadawy, *Corrosion*, 62 (2006) 293.
8. N. O. Eddy, *Electrochim. Acta*, 27 (2009) 579.
9. M. A. Quraishi, A. Singh, V. K. Singh, D. K. Yadav and A. S. Singh, *Mater. Chem. Phys.*, 122 (2010) 114.
10. M. Lebrini, F. Robert, A. Lecante and C. Roos, *Corros. Sci.*, 53 (2011) 687.
11. M. Znini, G. Cristofari, L. Majidi, A. Ansari, A. Bouyanzer, J. Paolini, J. Costa, and B. Hammouti, *Int. J. Electrochem. Sci.*, 7 (2012) 3959.
12. H. Cang, W. Y. Shi, J. L. Shao and Q. Xu, *Int. J. Electrochem. Sci.*, 7 (2012) 3726.
13. L. J. Li, X. P. Zhang, J. L. Lei, J. X. He, S. T. Zhang and F. S. Pan, *Corros. Sci.*, 63 (2012) 82.
14. K. M. Ismail, *Electrochim. Acta*, 52 (2007) 7811.
15. D. Q. Zhang, Q. R. Cai, X. M. He, L. X. Gao and G. D. Zhou, *Mater. Chem. Phys.*, 112 (2008) 353.
16. M. A. Amin, K. F. Khaled, Q. Mohsen and H. A. Arida, *Corros. Sci.*, 52 (2010) 1684.
17. H. Cang, W. Y. Shi, Y. Lu, J. L. Shao and Q. Xu, *Asian J. Chem.*, 24 (2012) 3675.
18. C. Deslouis, B. Tribollet, G. Mengoli and M. M. Musiani, *J. Appl. Electrochem.*, 18 (1998) 374.
19. O. E. Barcia, O. R. Mattos, N. Pebere and B. Tribollet, *J. Electrochem. Soc.*, 140 (1993) 2825.
20. P. Bommersbath, C. Alemany-Dumont, J. P. Millet and B. Normand, *Electrochem. Acta*, 51 (2006) 4011.
21. C. H. Hsu and F. Mansfeld, *Corrosion*, 57 (2001) 747.
22. S. Martinez and M. Metikos-Hukovic, *J. Appl. Electrochem.*, 33 (2003) 1137.
23. M. Lebrini, M. Lagrenée, M. Traisnel and Gengembre L, *Appl. Surf. Sci.*, 253 (2007) 9267.
24. Y. M. Tang, X. Y. Yang, and W. Z. Yang, *Corros. Sci.*, 52, (2010) 1801.
25. S. Xia, M. Qiu, L. Yu, F. Liu and H. Zhao, *Corros. Sci.*, 50 (2008) 2021.